



# From waste to packaging: Smart edible films from sericin and red cabbage for fruit coating

Daniela Pinheiro<sup>a,\*</sup>, Ana Rita Ferraz<sup>b,c,d</sup>, Sofia Esteves<sup>b</sup>, Ofélia Anjos<sup>c,d,e</sup>, Maximiano P. Ribeiro<sup>a</sup>

<sup>a</sup> BRIDGES - Biotechnology Research, Innovation and Design for Health Products, Polytechnic University of Guarda, Avenida Dr. Francisco Sá Carneiro, n.º 50, 6300-559, Guarda, Portugal

<sup>b</sup> School of Agriculture, Polytechnic University of Castelo Branco, 6001-909, Castelo Branco, Portugal

<sup>c</sup> CERNAS-IPCB - Research Center, Polytechnic University of Castelo Branco, Quinta da Senhora de Mércules, 6001-909, Castelo Branco, Portugal

<sup>d</sup> CBPBI - Plant Biotechnology Centre of Beira Interior, 6001-909, Castelo Branco, Portugal

<sup>e</sup> CEF - Forest Research Centre, School of Agriculture, University of Lisbon, 1349-017, Lisboa, Portugal

## ARTICLE INFO

### Keywords:

Edible films  
Sericin  
Red cabbage  
Food packaging  
Sustainability

## ABSTRACT

This study aimed to develop new smart edible films for fruit preservation and freshness monitoring using sericin, an undervalued by-product of the sericulture industry, and red cabbage extract (RC). The films were prepared using a sodium alginate matrix, and two sets of films were developed. One incorporating sericin, and other incorporating sericin and RC. Chemical and mechanical characterization showed that sericin improved film thickness, mechanical strength, and water retention. The films also exhibited acceptable water vapor transmission rates and swelling behavior, showing their suitability as coatings. The cytotoxicity was assessed prior to application, and no toxic effects were observed in human fibroblasts. When applied to blueberries, the coatings significantly reduced weight loss during storage at both room temperature and under refrigeration. Although no visible color changes were observed on the coated blueberries, the RC-containing films demonstrated clear pH-responsive color changes in laboratory tests, highlighting their potential as intelligent freshness indicators. Overall, the results demonstrate the dual functionality of these films as biodegradable protective coatings with indicator potential, offering a sustainable approach to reducing postharvest fruit losses and food waste.

## 1. Introduction

Plastics are present in almost every aspect of daily life, with the food industry dominating global plastic production. Although conventional plastics are lightweight, durable, and cost-effective, their fossil-fuel origin and poor biodegradability contribute significantly to environmental pollution. Growing concerns regarding plastic waste mismanagement and microplastic contamination have intensified the demand for biodegradable and sustainable alternatives to conventional food packaging that can preserve food quality while reducing environmental impact (Kumar et al., 2024).

Silk sericin, a protein traditionally regarded as waste in the silk reeling industry, represents a promising resource for sustainable innovation in food packaging. Typically removed during the degumming process, sericin accounts for approximately 15-35% of the cocoon's total weight and is commonly discharged into wastewater, significantly

contributing to its high organic load and environmental impact (Saad et al., 2023; Seo et al., 2023; C. Yang et al., 2023). Although traditionally regarded as a waste product, sericin possesses a unique biochemical profile characterized by a high content of hydrophilic amino acids, such as serine, glycine, and aspartic acid. These features confer excellent film-forming properties, water retention capacity, and inherent bioactivity, including antioxidant, antimicrobial, and ultraviolet (UV) protection effects (Aad et al., 2024; Meerasri et al., 2024; Oh et al., 2021; Pandey et al., 2024; Tarangini et al., 2022).

As a result, sericin has emerged as a valuable biopolymer for the production of edible films and surface coatings aimed at extending the shelf life of highly perishable foods and improving their safety. These sericin-based coatings are semi-permeable and can regulate the transfer of water vapor and gases, thereby helping to reduce water loss, oxidation, and microbial growth (Hailu et al., 2025; Hussain et al., 2024; Kavi et al., 2024; Seo et al., 2023; C. Yang et al., 2023). Therefore, the

\* Corresponding author.

E-mail address: [drpinheiro@ipg.pt](mailto:drpinheiro@ipg.pt) (D. Pinheiro).

<https://doi.org/10.1016/j.fbio.2026.108488>

Received 9 January 2026; Received in revised form 5 February 2026; Accepted 13 February 2026

Available online 14 February 2026

2212-4292/© 2026 The Authors. Published by Elsevier Ltd. This is an open access article under the CC BY license (<http://creativecommons.org/licenses/by/4.0/>).

incorporation of sericin in food packaging materials offers dual benefits: the valorisation of industrial by-products and the enhancement of sustainability and functional performance in agri-food packaging.

In addition, sericin has been investigated as a sustainable and low-cost protein source for developing fat-free edible films. These sericin-based coatings have shown promise in preserving the freshness of harvested fruits and vegetables. With consumer demand increasingly favoring fresh, minimally processed, nutrient-rich foods, reducing post-harvest losses has become a strategic priority for growers, distributors, and retailers.

In this context, the present study focuses on the development of a smart edible film for coating fresh blueberries, based on red cabbage extract (RC). RC is a widely available source of water-soluble flavonoid pigments, rich in anthocyanins that exhibit reversible color changes in response to pH. This property makes anthocyanins suitable for smart packaging systems, serving as visual indicators of a product's freshness. In addition to their pH sensitivity, anthocyanins possess strong antioxidant activity, contributing both to product protection and quality monitoring (Abedi-Firoozjah et al., 2022; Kosyvaki et al., 2022; Oladzabbasabadi et al., 2022; Roy & Rhim, 2021). By combining the protective properties of sericin with the pH-responsive nature of anthocyanins, this study aims to develop a film that extends the shelf life of blueberries while providing real-time spoilage monitoring.

Globally, the silk industry generates approximately 50,000 tons of sericin each year as a by-product of the degumming process (Arango et al., 2021; Seo et al., 2023), much of which is discarded despite its film-forming potential and biological activity. Several studies have shown that sericin-based films can enhance the preservation of various food products due to their antioxidant and antimicrobial properties (Aad et al., 2024; Apiwattanasiri et al., 2022; Chimvaree et al., 2019; Kavi et al., 2024; Meerasri et al., 2024). Biopolymer-based edible films, made from proteins such as sericin or polysaccharides, are expected to play a key role in the future of eco-friendly food packaging. They provide barrier properties against moisture and gases, enhance food safety, and degrade naturally after use (Behrooznia & Nourmohammadi, 2024; Metha et al., 2024; Nechita & Roman, 2020). These films can be produced economically using solvent casting or extrusion and can be easily applied to fruit surfaces by dipping or spraying (Atta et al., 2022; Bayram et al., 2021).

RC anthocyanins are particularly valued for their broad pH-responsive color range, shifting from red under acidic conditions (pH < 5) to blue or green at alkaline pH values (pH > 8). This pronounced chromatic sensitivity makes RC extract highly suitable for intelligent packaging applications aimed at freshness monitoring. In addition to their indicator function, RC-derived anthocyanins exhibit antioxidant and antimicrobial activities. Their successful incorporation into biopolymer matrices has been reported for monitoring spoilage in fish, shrimp, meat, milk, and other protein-rich foods (Abedi-Firoozjah et al., 2022; Ghareaghajlou et al., 2021).

In the fruit sector, blueberries (*Vaccinium* spp.) are particularly vulnerable to postharvest deterioration, even under refrigerated conditions, with a limited shelf life of 7 to 14 days. This vulnerability is due to their high respiration rate, delicate skin, and strong susceptibility to fungal and microbial contamination, which can lead to postharvest losses of up to 30% during transportation and retail distribution (Bof et al., 2021; Shi et al., 2024). Traditional coatings, such as chitosan or starch, can slow down deterioration but do not provide freshness indicators. Previous studies on smart films combining RC extract with biopolymers such as chitosan, gelatin, cellulose, and polyvinyl alcohol (PVA) have shown pH-sensitive color changes along with improved mechanical and barrier properties. However, to date, no study has investigated the combination of sericin and RC extract to produce a dual-function smart film specifically for fruit coating applications (Bof et al., 2021; Oladzabbasabadi et al., 2022; Roy et al., 2021; Shi et al., 2024).

In this context, the present study explores the valorisation of agro-

industrial by-products, specifically silk sericin and RC extract, through the development of a smart edible film designed for fruit coating applications. This work is based on the assumption that the intrinsic film-forming and barrier properties of sericin can be effectively combined with the pH-responsive behavior of anthocyanins, yielding a system that not only enhances fruit preservation but also provides visual information related to freshness. Recent studies have reported significant advances in active and intelligent edible films derived from biopolymers and natural pigments, underscoring their potential for sustainable food packaging and spoilage monitoring (Arshad et al., 2025; Iqbal et al., 2025). However, while sericin-based coatings have mainly focused on preservation performance, anthocyanin-based systems have been predominantly investigated as colorimetric indicators within smart packaging matrices. The integration of these two functionalities into a single edible coating, particularly for direct application to fresh fruits, remains largely unexplored.

To the best of our knowledge, no previous study has examined the combination of sericin and RC extract in a dual-function edible film specifically evaluated as a coating for blueberries. Therefore, this work aims to develop and characterize a sericin-based smart edible film that integrates mechanical stability, barrier performance, and pH-responsive behavior, and to evaluate its effectiveness in preserving blueberry quality under both room-temperature and refrigerated storage conditions. By simultaneously addressing fruit preservation and real-time freshness monitoring within a single material, this study advances the development of sustainable, multifunctional edible coatings for perishable fruit applications.

## 2. Materials and methods

### 2.1. Materials

Silkworm (*Bombyx mori*) cocoons were supplied by the Portuguese Association of Parents and Friends of Mentally Disabled Citizens (APPACDM) in Castelo Branco, Portugal. Sodium alginate was purchased from Panreac, calcium chloride dihydrate ( $\text{CaCl}_2 \cdot 2\text{H}_2\text{O}$ ) from Scharlab, and glycerol from Acofarma. Red cabbage (RC) and blueberries were bought from a local store. Sodium chloride and D-glucose were purchased from Labchem, potassium chloride from Honeywell, potassium phosphate monobasic from AMRESCO, ethylenediaminetetraacetic acid (EDTA) from Labkem, sodium bicarbonate from José Manuel Gomes Dos Santos Lda, and trypan blue from Alfa Aesar. Disodium hydrogen phosphate dihydrate and 3-(4,5-dimethyl-2-thiazolyl)-2,5-diphenyl-2H-tetrazolium bromide (MTT) were purchased from VWR. Trypsin, magnesium sulfate heptahydrate ( $\text{MgSO}_4 \cdot 7\text{H}_2\text{O}$ ), Dulbecco's modified eagle's medium (DMEM)-F12, fetal bovine serum (FBS), antibiotic-antimycotic solution ( $100 \times$ , stabilized), commercial sericin, and dimethyl sulfoxide (DMSO) were acquired from Sigma. Cryopreserved normal adult human dermal fibroblasts cells (NHDF) were purchased from PromoCell (Labclinics, S.A.; Barcelona, Spain). All reagents and solvents were used as received unless stated otherwise. Ultra-pure water (pH = 5.4) was purified using an Aquinity<sup>2</sup> P10 Ultra-Pure Water System.

### 2.2. Experimental procedures

#### 2.2.1. Extraction of silk sericin

After removing the silkworm from the cocoon's shells and properly cleaning them, the cocoons were weighed, cut into small pieces to help the extraction and, the degumming of silk was performed by high pressure and high temperature (HPHT, autoclave). Silk sericin was extracted with ultra-pure water (10 g of dry silkworm cocoon's and 250 mL of water) by autoclaving (VWR® Vapor-Lineco) at 120 °C for 60 min. The obtained solution was then filtered to remove the remaining cocoon shells, distributed into several vials, frozen at -80 °C and freeze-dried using a Telstar LyoQuest - 85 Plus to obtain silk sericin powder.

The remain cocoons shells were dried at room temperature (R.T.), and weighted for the calculation of the extraction yield (Eq. (1)) (Silva et al., 2012):

$$\text{Extraction Yield (\%)} = 1 - \left( \frac{W_f}{W_0} \right) \times 100 \quad (1)$$

where  $W_0$  corresponds to the initial weight of the cocoons and  $W_f$  corresponds to the final weight, after the silk sericin extraction, of the remain cocoons.

### 2.2.2. Extraction of the anthocyanins from red cabbage

Red cabbage (RC) leaves (100 g) were cut into small pieces and immersed in 200 mL of distilled water at 90 °C with magnetic stirring for 60 min. The solution was then filtered using filter paper, distributed into several vials, and frozen at -20 °C for future use.

### 2.2.3. Preparation of the films

Sodium alginate (2.0% (w/v)) was dispersed in 20 mL of purified water and homogenized for 20 min at 14,000 rpm using an ULTRA-TURRAX®-IKA (Norleq). The resulting mixture was transferred to a stirring plate at 90 °C under constant stirring, and glycerol (600 µL) was added and allowed to dissolve for 10 min. Calcium chloride (1.5 mL, 1.0 g/100 mL) was then added using a syringe pump (New Era Plus Systems, Inc., Model 300) to control the flow rate (1.5 µL/min) while maintaining the same temperature and stirring conditions. The obtained solution, designated SerAlg0 (base formulation), was poured into a Petri dish (90 mm diameter) and dried in an orbital shaker (Edmund Buhler GmbH) at 37 °C for 24 h. After drying, the films were peeled off and immersed in a calcium chloride solution (3.0 g/100 mL) for 5 min. The calcium chloride concentrations were based on Lopes et al. (Alves Lopes et al., 2020).

Three different formulations were prepared: SerAlg0 (base formulation), SerAlg1 (containing 0.5% (w/v) sericin), and SerAlg2 (containing 1.0% (w/v) sericin) (Table S1). Sericin was added after sodium alginate and before glycerol. Additionally, three more formulations incorporating RC extract were prepared by replacing 2.5 mL of purified water with the extract (resulting in 17.5 mL of purified water and 2.5 mL of extract). These formulations-SerAlgRC0, SerAlgRC1, and SerAlgRC2-are also summarized in Table S1. To ensure reproducibility, three replicates of each formulation were prepared.

### 2.2.4. Blueberries dip coating

Blueberries were dip-coated in the six formulations (SerAlg0, SerAlg1, SerAlg2, SerAlgRC0, SerAlgRC1, and SerAlgRC2). The formulations were first allowed to cool to R.T. (22 °C) before use. Each dipping step lasted for 10 s, followed by drying for 10 min at R.T. The coated blueberries were then submerged in a CaCl<sub>2</sub>·2H<sub>2</sub>O solution (3.0 g/100 mL) for 5 min and dried at R.T. for 10 min.

The weight of the blueberries was recorded before and after the dipping process described above. For each formulation, a control sample without dipping (no coating) was also included. The samples were then divided into two groups: one stored under refrigeration (4 °C) and the other at R.T.

For each formulation, three blueberries were used, and the entire procedure was performed in triplicate to ensure reproducibility. During the experiment, the blueberries were weighed and photographed daily for the first week and then weekly for a month. The fraction of original weight (%) was calculated (Eq. (2)):

$$\text{Fraction of original weight (\%)} = \frac{\text{Weight at time } t}{\text{Initial weight}} \quad (2)$$

where *Weight at time t* is the weight of the blueberries at a specific time point, and the *Initial weight* is the weight of the blueberries at the start of the experiment (before any treatments or time have passed).

## 2.3. Chemical and mechanical sericin-based films characterization

### 2.3.1. Ultraviolet-visible (UV-Vis) spectroscopy

UV-Vis silk sericin spectra were acquired on a Thermo Scientific Multiskan GO Microplate UV-Vis spectrophotometer with a 1 cm quartz cuvette over the range 220-320 nm at R.T. (22 °C). For comparison, the UV-Vis spectrum of commercial sericin was also obtained under the same conditions.

### 2.3.2. FTIR-ATR characterization of sericin and sericin-based film

Fourier transform infrared spectroscopy with attenuated total reflection (FTIR-ATR) was used to acquire the spectra of extracted and commercial sericin. This was done using a Thermo Scientific Nicolet iS10 FTIR spectrometer (Thermo Fisher Scientific, USA), which was equipped with a Smart iTR accessory. The apparatus was operated using the Omnic software package from Thermo Fisher Scientific, Inc. (version 9.2.28). A total of 180 scans were performed at a resolution of 4 cm<sup>-1</sup> in the range of 4000-500 cm<sup>-1</sup>.

The FTIR-ATR spectra of sericin-based films were obtained using a Bruker spectrometer (Alpha, Bruker Op-tics GmbH, Ettlingen, Germany), which was equipped with a diamond crystal. Five spectra per sample were collected, each comprising 32 scans at a resolution of 4 cm<sup>-1</sup> within 4000-400 cm<sup>-1</sup> range. Background measurements were performed prior to scanning a sequence of five samples. The system was operated using the OPUS 8.5.29 software provided by the manufacturer. All spectra were acquired at R.T.

### 2.3.3. Thickness ( $\delta$ )

The film thickness was measured at 10 different positions using a micrometer (0.001 mm, Digimatic Micrometer MDC-25P; Mitutoyo, Tokyo, Japan). At least three replicates were considered for each formulation.

### 2.3.4. Color determination

The color properties of the films were determined using the Commission Internationale d'Éclairage (CIE) 1976 L\*a\*b\* color coordinates system, where L\* represents lightness (0 = black, 100 = diffuse white), a\* indicates the red-green balance (+a\* = red and -a\* = green hues), and b\* corresponds to the yellow-blue balance (+b\* = yellow and -b\* = blue). Measurements were performed using a Chroma Meter CR-400 Konica Minolta (Osaka, Japan). The reported L\*, a\* and b\* values represent the mean of three measurements taken at different locations on each film, with a relative standard deviation lower than 2%. Additionally, the film color variation ( $\Delta E^*$ ) was calculated using Eq. (3) (Chentir et al., 2024):

$$\Delta E^* = \sqrt{(\Delta L^*)^2 + (\Delta a^*)^2 + (\Delta b^*)^2} \quad (3)$$

where  $\Delta L^*$ ,  $\Delta a^*$  and  $\Delta b^*$  are differences between the corresponding color parameter of the sericin-based films and that of base formulation film.

### 2.3.5. Density determination

The apparent density ( $\rho$ ) of the film samples was determined by measuring their weights, lengths, widths, and thickness using weighing balance, ruler, and thickness gauge, respectively. All measurements were repeated three times. It was calculated using Eq. (4), with results expressed in g/cm<sup>3</sup> (Rodrigues et al., 2021):

$$\rho = \frac{\text{Weight}}{\text{Length} \times \text{Width} \times \text{Thickness}} \quad (4)$$

### 2.3.6. Mechanical properties

Tensile strength (TS), elongation at break (EAB), and Young's modulus (YM) were measured using a Texture Analyzer (TA-XT Plus, Stable Micro Systems, Godalming, UK). Measurements were performed

in triplicate for each formulation. Each test strip was cut to a specific size (45 mm × 10 mm) and placed longitudinally in a tensile grip probe (A/MTG). The initial grip separation was set to 5 mm, and the crosshead speed was 8.30 s. The test was concluded when the film broke.

Tensile strength (TS) was calculated using Eq. (5), with results expressed in MPa (Rodrigues et al., 2021):

$$TS = \frac{\text{Force at break}}{\text{Thickness} \times \text{width}} \quad (5)$$

Elongation at break (EAB) was determined using Eq. (6) (Rodrigues et al., 2021):

$$EAB(\%) = \frac{\text{Increase in length}}{\text{Original length}} \times 100 \quad (6)$$

Young's modulus (YM) was calculated using Eq. (7), with results expressed in MPa:

$$YM = \frac{\text{Stress}}{\text{Strain}} = \frac{\text{Force} \times \text{length}}{\text{Extension} \times \text{Area}} \quad (7)$$

### 2.3.7. Water vapor transmission rate (WVTR)

Water vapor diffusion through the films was evaluated as described elsewhere (Miguel et al., 2017). Briefly, the films were used to seal the opening of a tube (1.5 cm<sup>2</sup>) containing 10 mL of ultrapure water. Parafilm tape was applied to secure the film to the tube. The sealed tubes were then incubated at 37 °C, and water loss was measured at specific time points (0 h (initial weight), 2 h, 4 h, 6 h, 8 h, 10 h, and 24 h) by determining the weight loss. An unsealed tube was used for the control test, and the measurements were repeated three times and performed in triplicate for each formulation. The water vapor transmission rate (WVTR) was obtained using Eq. (8):

$$WVTR = \frac{W_{\text{loss}}}{A} \quad (8)$$

where  $W_{\text{loss}}$  is the daily weight loss of water and  $A$  is the area of the tube test (m<sup>2</sup>).

### 2.3.8. Swelling profile

Each film sample (2 cm × 2 cm) was weighed and placed in a tube with 10 mL of purified water. The tubes were then incubated at 37 °C in an orbital shaker at 100 rpm for 30 min. After that time, the surface of each sample was carefully wiped with filter paper, to remove excess of water, and the final weight was measured. This process was performed eight times over 24 h, with measurements recorded at 30 min, 1 h, 2 h, 3 h, 6 h, 8 h, 21 h, and finally 24 h. All measurements were repeated three times. The swelling ratio was determined using Eq. (9) (Miguel et al., 2023):

$$\text{Swelling} (\%) = \frac{W_t}{W_o} \times 100 \quad (9)$$

where  $W_t$  is the final weight, and  $W_o$  is the initial weight of the films.

## 2.4. Cell viability test

### 2.4.1. Cytotoxic assay

Following the guidelines of the International Organization for Standardization (ISO 10993-5) the cytotoxic profile of the films was measured using the MTT assay. A small piece of the film, covering a quarter of the well surface, was placed in each well of a sterile 96-well plate. Prior to cell culture, the films were sterilized under UV light for 45 min and washed with culture medium. NHDF were seeded at densities of  $3 \times 10^4$ ,  $1 \times 10^4$ , and  $2 \times 10^3$  cells/well and incubated at 37 °C in a humidified 5% CO<sub>2</sub> atmosphere for 24, 72, and 168 h, respectively. After each incubation period, the culture medium was removed and replaced with 50 μL of MTT solution (5.0 mg/mL), followed by a 4 h incubation at 37 °C in a 5% CO<sub>2</sub> atmosphere. The cells were then treated

with 100 μL of DMSO and placed in an orbital shaker (shaker incubador Edmund Bühler) at 37 °C, 80 rpm for 30 min. The absorbance of each sample ( $n = 6$ ) was measured at 570 nm using a Thermo Scientific Multiskan GO UV-Vis microplate spectrophotometer. Cells incubated with 96% ethanol served as the positive control (K<sup>+</sup>), while cells incubated with culture medium alone served as the negative control (K<sup>-</sup>). Cell growth was monitored with an Optika inverted light microscope equipped with an Optikam B5 digital camera (Bergamo, Italy).

### 2.4.2. Color response to pH changes

Sericin-alginate films incorporated with RC extract (1 cm × 1 cm) were immersed in buffer solutions of pH 2, 4, 6, 8, 10, and 12. The resulting color changes of the films were then photographed.

### 2.4.3. Statistical analysis

The results are expressed as the mean ± standard deviation (SD). Differences between groups were evaluated using a one-way analysis of variance (ANOVA), followed by Tukey's post hoc test, unless otherwise specified. Statistical significance was defined as  $p < 0.05$ . All statistical analyses were performed out using GraphPad Prism version 8.01 for Windows (GraphPad Software, San Diego, California, USA).

## 3. Results and discussion

### 3.1. Evaluation of the extracted sericin

A  $28 \pm 1.73\%$  extraction yield was achieved using the HPHT method, aligning with literature values (Bascou et al., 2022). The UV-Vis and FTIR-ATR spectra of commercial and HPHT-extracted sericin (Fig. S1 and S2) confirmed their structural similarity. The UV-Vis spectra (Fig. S1) showed two characteristic peaks: 230 nm (peptide bonds) and 275 nm (aromatic amino acids), consistent with  $\pi \rightarrow \pi^*$  transitions (Gupta et al., 2014; Hossain et al., 2023; Seo et al., 2023). The FTIR-ATR spectra (Fig. S2) exhibited bands at 1644 cm<sup>-1</sup> (amide I, random coil, C=O stretching) (Hossain et al., 2023), 1515 cm<sup>-1</sup> (amide II,  $\beta$ -sheets, N-H bending) (Pan, Jin, et al., 2024), and 1238 cm<sup>-1</sup> (amide III, random coil, C-N stretching, N-H bending) (Aramwit et al., 2010). The peaks at 3281 cm<sup>-1</sup> and 2934 cm<sup>-1</sup> correspond to amide A and C-O stretching of carboxylic groups, respectively (Bascou et al., 2022; Jaya Prakash et al., 2022). These findings confirm that HPHT-extracted sericin retains its native protein composition and secondary structure, closely resembling that of commercial sericin.

### 3.2. Analysis of the visual aspect of the films

The visual appearance of bio-based packaging films is important not only for consumer perception but also for their functional and commercial applications. To assess the effect of incorporating sericin and RC extract on the visual properties of alginate-based films, color parameters were measured using the CIE 1976 L\*a\*b\* color system. The visual differences observed in the films (Fig. 1 and Fig. S3) were supported by the CIE 1976 L\*a\*b\* color coordinates and the total color difference ( $\Delta E^*$ ), as shown in Fig. 2 and Table S2. Films without RC extract (SerAlg0-SerAlg2) exhibited a gradual decrease in lightness (L\*) as sericin content increased from 0 to 1.0% (w/v), with values ranging from  $90.21 \pm 1.54$  to  $88.48 \pm 0.85$ . This trend indicates slight film darkening and is consistent with the increased surface turbidity and opacity observed in Fig. 1A–C and Fig. S3A–B. Simultaneously, the b\* coordinate increased significantly from  $5.71 \pm 0.13$  (SerAlg0) to  $12.04 \pm 0.62$  (SerAlg2), indicating a shift toward more yellowish tones (Fig. 2). The corresponding  $\Delta E^*$  values (1.30–6.43) reflect moderate but noticeable visual differences that become more pronounced with higher sericin content. In contrast, incorporation of RC extract (SerAlgRC0-SerAlgRC2) resulted in more pronounced changes in both lightness and chromaticity. The L\* values decreased significantly from  $76.94 \pm 0.60$  (SerAlgRC0) to  $57.56 \pm 0.99$  (SerAlgRC2), corresponding to the visible darkening and

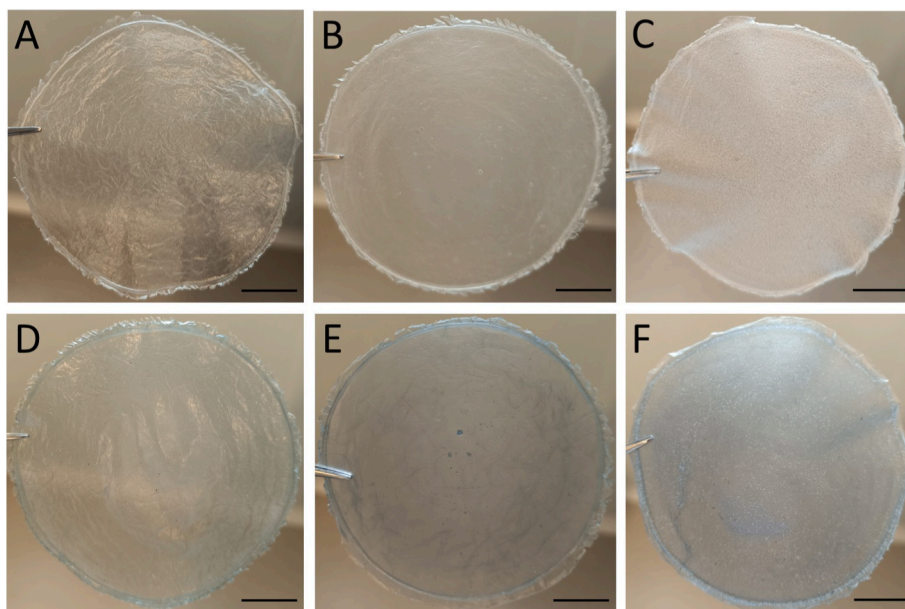


Fig. 1. Photographs of the films: SerAlg0 (A), SerAlg1 (B), SerAlg2 (C), SerAlgRC0 (D), SerAlgRC1 (E), and SerAlgRC2 (F). The scale bar is 1.0 cm.

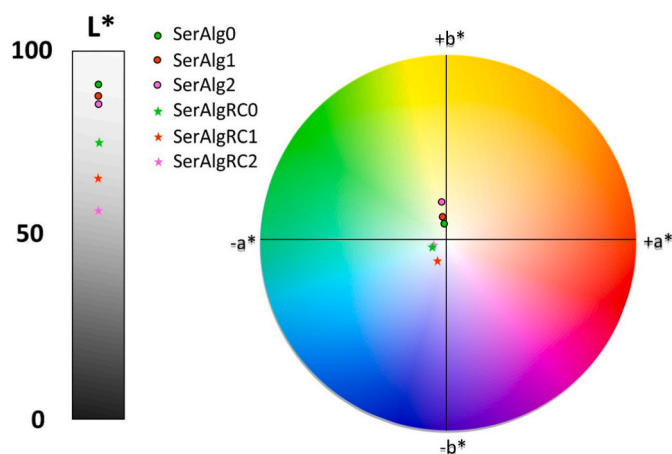


Fig. 2. CIE 1976 L\*a\*b\* color diagram: SerAlg0 (green-filled circle), SerAlg1 (red-filled circle), SerAlg2 (pink-filled circle), SerAlgRC0 (green star), SerAlgRC1 (red star), and SerAlgRC2 (pink star).

increased opacity shown in Fig. 1D–F and Fig. S3C–D. The  $a^*$  values shifted toward more negative values (e.g., from  $-0.53 \pm 0.01$  in SerAlg0 to around  $-4.70 \pm 0.08$  in SerAlgRC0), indicating greener tones, while  $b^*$  values became negative, suggesting bluish coloration (Fig. 2). These results are consistent with the known pH-dependent color behavior of anthocyanins at neutral to slightly basic conditions (Ghareaghajlou et al., 2021). Overall, these chromatic changes resulted in higher  $\Delta E^*$

values (up to  $33.98 \pm 8.87$ ), highlighting the strong visual impact of RC anthocyanins and their interaction with the sericin-alginate matrix.

### 3.3. Film thickness and apparent density

The thickness of the films was evaluated to assess the influence of sericin and RC extract on the structural properties of the alginate-based formulations. Film thickness ranged from  $0.112 \pm 0.011$  mm to  $0.182 \pm 0.022$  mm (Table 1). All formulations exhibited thickness values within the acceptable range for edible films ( $\leq 0.25$  mm), confirming their suitability for food packaging or coating applications (Suresh et al., 2022). As shown in Fig. 3 and Table 1, the control films without sericin (SerAlg0 and SerAlgRC0) presented the lowest thickness values ( $\approx 0.11$  mm), while the incorporation of sericin resulted in a concentration-dependent increase in film thickness. This effect was observed regardless of the presence of RC extract and may be attributed to enhanced molecular entanglement and increased solution viscosity during film formation. Similar trends have been reported for sericin-containing biopolymer films in previous studies (Hailu et al., 2025).

Regarding apparent density, Table 1 shows an increase with the incorporation of sericin and RC extract. This increase can be attributed to stronger molecular interactions, such as hydrogen bonding and hydrophobic interactions, between alginate, sericin, and the phenolic compounds present in RC. These interactions likely promote more compact chain packing, reduce porosity, and result in denser films. Comparable effects have been reported for other biopolymer systems incorporating polyphenols or protein-based components (Riaz et al.,

Table 1

Thickness, apparent density, water vapor transmission rate (WVTR), tensile strength (TS), elongation at break (EAB), and Young's modulus (YM) of the sericin-alginate films.

Formulations	Thickness ( $\delta$ ) (mm)	Density ( $\rho$ ) (g/cm <sup>3</sup> )	WVTR (g/m <sup>2</sup> /day)	Tensile strength (TS) MPa	Elongation at break (EAB) (%)	Young's modulus (YM) MPa
SerAlg0	$0.11 \pm 0.007$	$0.07 \pm 0.002$	$1314 \pm 20$	$11.26 \pm 1.06$	$7.28 \pm 1.00$	$13.22 \pm 1.76$
SerAlg1	$0.12 \pm 0.012$	$0.09 \pm 0.015$	$1135 \pm 45$	$14.06 \pm 0.84$	$4.08 \pm 1.61$	$15.94 \pm 1.35$
SerAlg2	$0.18 \pm 0.022$	$0.11 \pm 0.007$	$1078 \pm 25$	$10.58 \pm 1.28$	$4.78 \pm 1.28$	$13.77 \pm 1.26$
SerAlgRC0	$0.11 \pm 0.011$	$0.09 \pm 0.017$	$1006 \pm 60$	$23.93 \pm 1.09$	$7.26 \pm 1.36$	$14.52 \pm 1.51$
SerAlgRC1	$0.12 \pm 0.006$	$0.10 \pm 0.010$	$972 \pm 98$	$19.14 \pm 1.70$	$8.23 \pm 1.17$	$15.36 \pm 1.42$
SerAlgRC2	$0.18 \pm 0.026$	$0.12 \pm 0.0004$	$961 \pm 53$	$15.43 \pm 2.01$	$5.82 \pm 0.56$	$13.03 \pm 1.00$

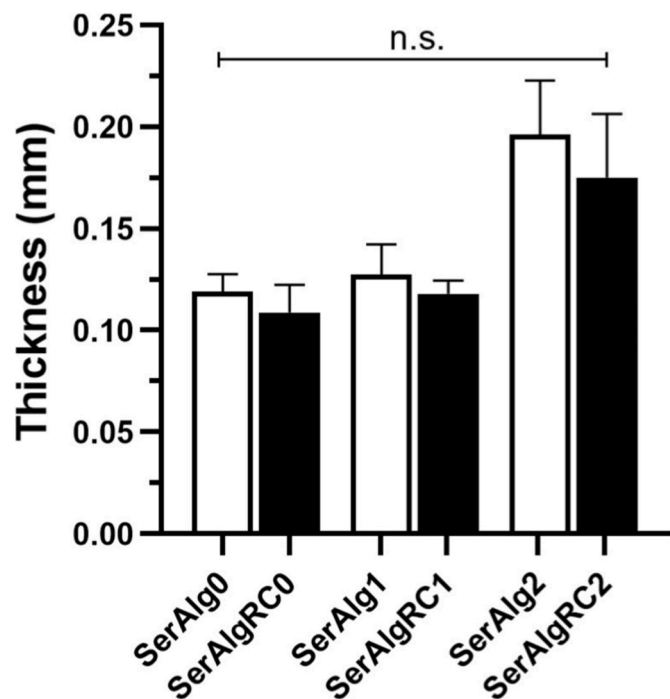


**Fig. 3.** Thickness of sericin-alginate films without (white bars) and with RC extract (black bars) as a function of sericin concentration. Data are presented as mean  $\pm$  standard deviation,  $n = 10$ . No statistically significant differences (n.s.) were observed between groups ( $p > 0.05$ ) for all pairwise comparisons.

2018).

### 3.4. FTIR-ATR analysis of the films

The FTIR-ATR spectra provided insight into the molecular interactions occurring within the sericin-alginate coatings, with and without the incorporation of RC extract. Commercial sericin was used as a reference standard.

As shown in Fig. 4A, the pure sericin spectrum (green line) displayed the characteristic amide bands—amide I ( $\sim 1617\text{ cm}^{-1}$ ), amide II ( $\sim 1520\text{ cm}^{-1}$ ), and amide III ( $\sim 1241\text{ cm}^{-1}$ )—associated with C=O, N–H, and C–N vibrations, which are useful for identifying this compound in the films. Similar FTIR-ATR peak patterns for pure sericin were reported by Saha et al. (Saha et al., 2019). In contrast the spectrum of sodium alginate (red line) exhibited a broad absorption band at  $\sim 3270\text{ cm}^{-1}$ , corresponding to O–H stretching vibrations typical of hydrophilic polysaccharides. The peaks at  $1603$  and  $1409\text{ cm}^{-1}$  were assigned to the asymmetric and symmetric stretching of carboxylate groups ( $-\text{COO}^-$ ), respectively.

FTIR-ATR analysis was performed with the aim of developing a quality control methodology for sericin-based edible coatings. Fig. 4B shows the FTIR-ATR spectra of the sericin-based coatings, highlighting the spectral bands associated with the vibrational modes of the characteristic functional groups of the matrix. The analyzed samples exhibited peaks in the regions of  $3500\text{--}2800\text{ cm}^{-1}$  and  $1750\text{--}700\text{ cm}^{-1}$ . A pronounced peak at  $3283\text{ cm}^{-1}$  was attributed to O–H stretching vibrations, mainly attributed to the water content in the sample, while the peaks at  $2926$  and  $2883\text{ cm}^{-1}$  were assigned to the asymmetric and symmetric stretching vibrations of C–H bonds in aliphatic  $-\text{CH}_2/-\text{CH}_3$  groups from amino acid side chains, such as alanine, valine, leucine, and isoleucine (M. Pan, Li, et al., 2024). For the coatings containing RC extract (SerAlgRC0, SerAlgRC1, SerAlgRC2), Fig. 4B also shows minor spectral shifts and intensity variations between  $1617$  and  $1030\text{ cm}^{-1}$ , that are ascribed to the interactions between phenolic compounds, mainly anthocyanins, and the sericin-alginate matrix. These hydrogen bonding and  $\pi\text{--}\pi$  stacking interactions likely contribute to a more cohesive and structurally stable polymeric network, consistent with the

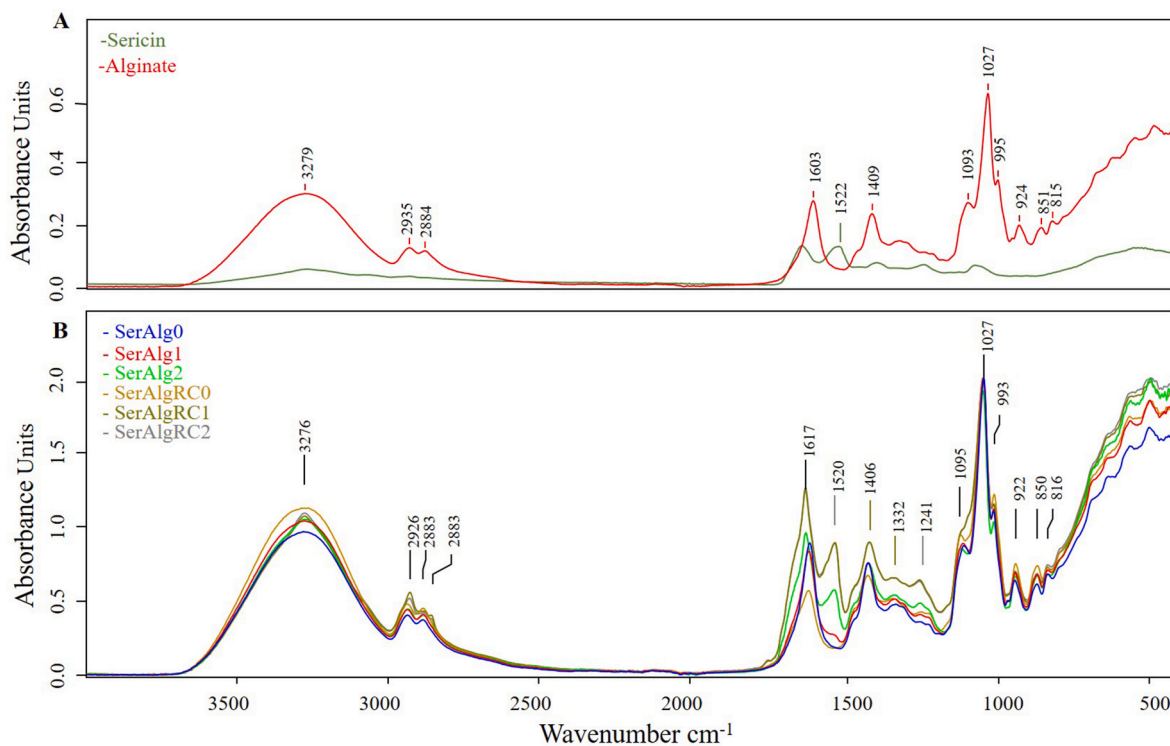


**Fig. 4.** FTIR-ATR spectra of (A) pure sericin and sodium alginate powders, and (B) composite coatings containing different sericin concentrations and red cabbage (RC) extract: SerAlg0 (base formulation), SerAlg1 (0.5% w/v sericin), SerAlg2 (1.0% w/v sericin), SerAlgRC0, SerAlgRC1, and SerAlgRC2 (formulations with 2.5 mL RC extract replacing purified water).

improved antioxidant and barrier properties observed in phenolic-enriched biopolymer systems (Zhang et al., 2024; Zhou et al., 2022). Although the peak at  $1519\text{ cm}^{-1}$  is characteristic of pure sericin and confirms the presence of N–H bending, symmetric C=O stretching was also observed around  $1405\text{ cm}^{-1}$ .

The results show that the sericin-alginate films successfully incorporate sericin into the alginate matrix. Changes in peak intensity or position, especially in the regions of amide I (C=O stretch at  $1650\text{ cm}^{-1}$ ) and amide II (N–H bending and C–N stretch at  $1530\text{ cm}^{-1}$ ), indicate interactions between sericin and alginate, such as hydrogen bonding.

These spectral findings were corroborated by principal component analysis (PCA) as shown in Fig. 5. PCA is a multivariate statistical method used to qualitatively distinguish structural differences among sericin-based coating formulations. The analysis was performed in the spectral range  $4000\text{--}400\text{ cm}^{-1}$ , following the application of various spectral pre-processing steps.

The first principal component (PC1), accounting for 76% of the total variance, clearly differentiated films without RC extract (SerAlg0–SerAlg2) from those containing RC (SerAlgRC0–SerAlgRC2), indicating chemical modifications induced by the incorporation of phenolic compounds. The second principal component (PC2), responsible for 18% of the total variance, was associated with increasing sericin content within the matrices. Loading plots revealed that the most influential spectral regions were located around  $\sim 1600\text{ cm}^{-1}$  (amide I) and  $\sim 1030\text{ cm}^{-1}$  (C–O), confirming that interactions among sericin, alginate, and phenolic compounds played a key role in differentiating the formulations. The PCA performed with FTIR-ATR spectra demonstrated that both sericin concentration and RC extract addition significantly influence the chemical composition and molecular organization of the sericin-alginate matrices, potentially affecting their functional and structural performance as edible coatings.

### 3.5. Mechanical properties

The evaluation of mechanical properties is essential to assess the resistance of packaging films to physical damage during transport, storage, and handling. As shown in Table 1, for sericin-based films without RC extract (SerAlg0–SerAlg2), the incorporation of 0.5% (w/v) sericin (SerAlg1) improved both TS and YM compared to the base formulation (SerAlg0). This enhancement is attributed to the formation of intermolecular hydrogen bonds between sericin and the alginate matrix, resulting in a more compact polymer network. Similar effects have been reported for sericin incorporation into flaxseed mucilage, elastin/collagen matrices (Hailu et al., 2025), and polysaccharide-protein biofilms made from aqueous wheat proteins and alginate solutions (Bishnoi et al., 2022). However, increasing the sericin content to 1.0% w/v (SerAlg2) led to a reduction in both TS and YM

relative to SerAlg1. This decrease may result from an excessive number of hydrogen bonding sites and potential phase incompatibility between sericin and alginate, which can disrupt network homogeneity and cohesion, leading to a less compact and mechanically weaker structure. Similar behavior has been reported in covalently cross-linked polymer networks, where high hydrogen bond density enhances stiffness but limits chain mobility and stretch ability, ultimately compromising mechanical integrity (Huang et al., 2021). In the present system, a high sericin concentration likely produced a rigid and disordered network, leading to reduced mechanical performance.

The incorporation of RC extract significantly improved the TS, with values increasing by 1.5–2.1 times compared to the corresponding RC-free films. The most pronounced enhancement was observed for SerAlgRC0 ( $23.93 \pm 1.09\text{ MPa}$ ), which exhibit an approximately 2.1-fold increase relative to SerAlg0 ( $11.26 \pm 1.06\text{ MPa}$ ) (Table 1). This improvement is attributed to anthocyanins present in RC extract, whose polyhydroxylated structure enables hydrogen bonding with hydrophilic functional groups (e.g., hydroxyl and amino groups) present in polysaccharides (such as alginate), proteins, and plasticizing agents. These interactions promote a denser and more cohesive polymer network, thereby improving the mechanical strength of the film. Similar improvements have been reported for films containing anthocyanin-rich extracts (Jamróz et al., 2019; Qin et al., 2019; Yong & Liu, 2020).

Despite the ability of sericin to interact with anthocyanins and alginate, increasing sericin content in RC-containing films (SerAlgRC1 and SerAlgRC2) did not further improve in TS. Instead, a progressive decrease in TS was observed compared to SerAlgRC0. This reduction may be attributed to competition for hydrogen bonding sites, disruption of optimal polymer-phenolic interactions, or the formation of structural irregularities caused by excess sericin, ultimately weakening the film network.

Overall, the TS values of the developed films were comparable to those of conventional food packaging materials, such as low-density polyethylene (LDPE, 8–10 MPa) and ethylene-vinyl alcohol copolymer (EVOH, 6–19 MPa), highlighting their potential applicability in packaging systems (Hailu et al., 2025).

YM followed trends similar to TS and showed relatively minor variations among formulations, indicating that RC extract had a limited effect on film stiffness (Table 1). In contrast, EAB tended to increase in the presence of RC extract, particularly for SerAlgRC1 ( $8.23 \pm 1.17\%$ ), suggesting enhanced molecular mobility. This behavior is likely related to the plasticizing effect of anthocyanins, which can disrupt intermolecular interactions and increase chain flexibility, as previously reported (Khan et al., 2024; Zhai et al., 2017). Notably, SerAlg0 ( $7.28 \pm 1.00\%$ ) and SerAlgRC0 ( $7.26 \pm 1.36\%$ ) also exhibited relatively high EAB values, indicating that the absence of sericin may favor a more flexible network due to reduced intermolecular densification. In contrast,

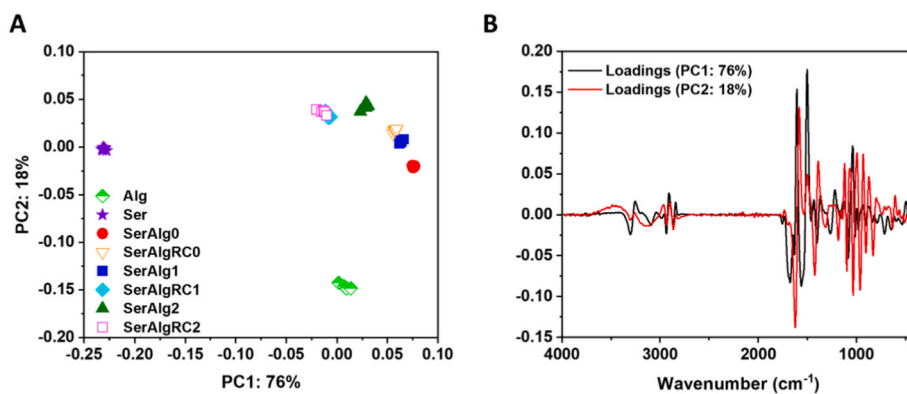


Fig. 5. Principal Component Analysis (PCA) and corresponding loading plots of FTIR-ATR data of sericin-based coatings. (A) PCA score plot illustrating the distribution of the six coating formulations (SerAlg0, SerAlg1, SerAlg2, SerAlgRC0, SerAlgRC1, and SerAlgRC2). (B) Loading plot of sericin-based films using spectra transformed by the first derivative Savitzky–Golay algorithm.

increasing sericin content to 1.0% (SerAlg2 and SerAlgRC2) reduced EAB, likely due to increased stiffness from enhanced bonding and reduced chain mobility. These results suggest that mechanical flexibility depends on both anthocyanin content and sericin concentration, with moderate sericin and the presence of RC extract enhancing flexibility, while higher sericin content reduces it.

### 3.6. Water vapor transmission rate

Fruits are characterized by high-water content and active metabolism, which continue after harvest. This leads to continuous water loss through the peel by transpiration, causing weight reduction, shriveling, and overall loss of quality. To mitigate these effects, edible coatings or films are commonly applied as postharvest treatments. These materials act as semi-permeable barriers that regulate gas and moisture exchange, slowing down transpiration and respiration. By reducing water vapor loss, coatings help preserve fruit appearance, texture, and firmness, thereby extending shelf life (Bof et al., 2021; Shi et al., 2024).

WVTR is a key parameter for evaluating the performance of such coatings. It quantifies the amount of water vapor that permeates through a unit area of the film under specific conditions and reflects the coating's ability to maintain the fruit's internal moisture. A WVTR within an appropriate range helps preserve a favourable microenvironment, minimizing both excessive dehydration and moisture accumulation, which can lead to texture degradation or microbial growth (Al-Harrasi et al., 2022; Otoni et al., 2017; J. Pan, Li, et al., 2024). Table 1 and Fig. 6, present the WVTR values of sericin-based films with and without RC. The results showed a clear decreasing trend with the incorporation of sericin into alginate-based films. SerAlg0 exhibited the highest WVTR value ( $1314 \pm 20$  (g/m<sup>2</sup>)/day), reflecting limited barrier performance. As sericin content increased (SerAlg1 and SerAlg2), WVTR decreased to  $1135 \pm 45$  and  $1078 \pm 25$  (g/m<sup>2</sup>)/day, respectively, indicating that sericin contributes to a more compact and less permeable matrix. This effect is likely due to the hydrophilic nature of sericin, which contains polar functional groups, such as hydroxyl (-OH), amino (-NH), and carboxyl (-COOH) that form hydrogen bonds with water molecules, retaining water within the polymer network and reducing vapor mobility (Sothornvit & Chollakup, 2009). Similar trends were observed in whey protein-sericin blended films, where increasing sericin from 0 to 0.1% caused a rapid 1.9-fold decrease in water vapor permeability, with a slower decline at higher concentrations, further supporting sericin's role in enhancing barrier properties (Wang et al., 2010).

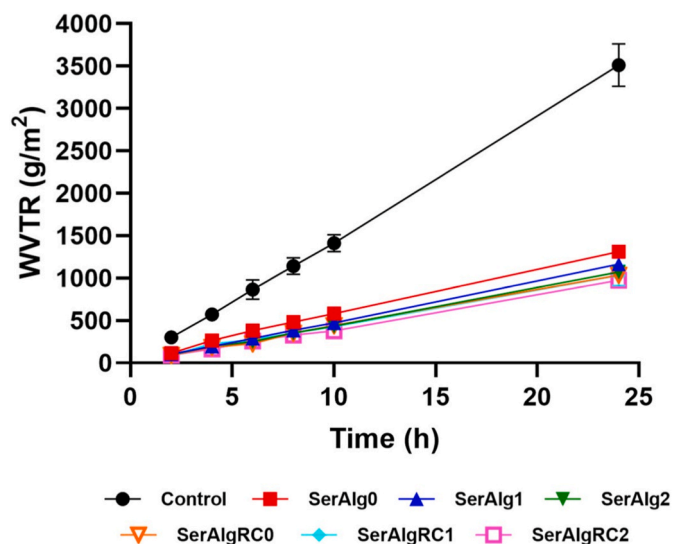


Fig. 6. Water vapor transmission rate of sericin-based films as a function of time.

The incorporation of RC extract (SerAlgRC0-SerAlgRC2) further improved water resistance, with SerAlgRC2 (highest sericin content) achieving the lowest WVTR value ( $961 \pm 53$  (g/m<sup>2</sup>)/day). These findings suggest a synergistic interaction between sericin and polyphenolic in RC extract, likely driven by enhanced hydrogen bonding and matrix densification, which effectively limit water vapor diffusion. Similar effects have been reported for alginate films containing tannic acid or tea polyphenols, where strong hydrogen bonding led to more compact internal network structure and reduced water vapor permeability (Dou et al., 2018; Li et al., 2022).

### 3.7. Swelling degree

Swelling is a key indicator of a film's ability to retain its structural integrity in aqueous environments. The swelling profiles of the sericin-based films are presented in Fig. 7. All formulations exhibited a rapid initial increase in swelling, reaching near-equilibrium within the first hour, which is a characteristic of hydrophilic polymeric matrices. Films without sericin (SerAlg0 and SerAlgRC0) showed limited water uptake capacity. In contrast, the incorporation of sericin into the alginate matrix significantly increased the swelling degree, with SerAlg2 and SerAlgRC2 reaching the highest values of  $323.35 \pm 3.30\%$  and  $356.97 \pm 14.14\%$ , respectively (Fig. 7 and Table S3). This increase is attributed to the abundance of hydrophilic functional groups in sericin (e.g., hydroxyl, carboxyl, and amino), which promote water absorption through hydrogen bonding. A similar trend was observed in electrospun nanofibers composed of polyvinyl alcohol, chitosan, and sericin (PVA/CHT/SS), where materials without sericin exhibited swelling ratios of approximately 325%, while those with higher sericin content reached up to 650% (Arango et al., 2021). Increased water absorption due to hydrophilic components has also been reported for membranes and hydrogels (Miguel et al., 2017).

The incorporation of RC extract (SerAlgRC1 and SerAlgRC2) further enhanced swelling. These results suggest that combining RC extract with higher sericin content increases film hydrophilicity and may reduce network density, allowing greater water uptake (Abedi-Firoozjah et al., 2022). This behavior is consistent with previous literature, for example, Pourjavaher et al. (Pourjavaher et al., 2017) and Kuswandi et al. (Kuswandi et al., 2020) reported that RC extract or its anthocyanins increased moisture absorption in bacterial cellulose-based membranes by disrupting polymer compactness and creating additional free volume.

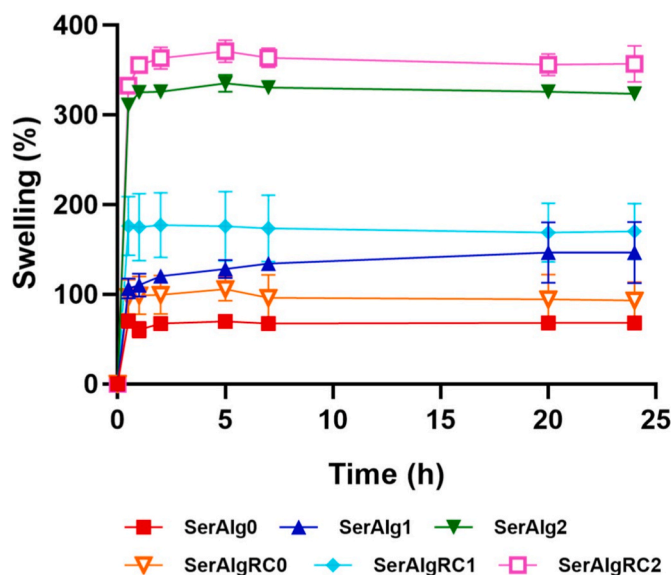


Fig. 7. Swelling profile of the produced films: SerAlg0, SerAlg1, SerAlg2, SerAlgRC0, SerAlgRC1 and SerAlgRC2.

Similarly, Maftoonazad and Ramaswamy (Maftoonazad & Ramaswamy, 2019) observed increased moisture absorption in PVA nanofibers containing RC extract, attributed to reduced intermolecular interactions caused by polyphenolic compounds.

These results indicate that swelling increased with higher sericin content and the incorporation of RC extract, showing that film composition can be used to modulate water absorption and tailor hydrophilicity for edible coating or moisture-sensitive packaging applications.

### 3.8. Evaluation of the cytotoxic profile of the films

Cytotoxic evaluation of packaging materials is essential to ensure their safety for food contact applications. In this study, the MTT assay was used to assess the viability of human fibroblast cells cultured in the presence of films containing increasing amounts of sericin, with and without RC extract, after 24, 72, and 168 h of incubation (Fig. 8 and Fig. S4). The results showed that none of the film formulations, whether supplemented with RC extract (Fig. 8B) or not (Fig. 8A), induced cytotoxic effects on human cells. These findings suggest that the developed films are non-cytotoxicity and hold promise and safe materials for food packaging applications.

### 3.9. Blueberries dip coating and evaluation of blueberries freshness

The postharvest preservation of blueberries was evaluated by applying edible coatings based on sericin-alginate films. The visual appearance of blueberries during storage under different coating conditions is shown in Fig. 9. At R.T. (Fig. 9A), uncoated blueberries exhibited noticeable dehydration and surface wrinkling by day 5, which progressed to fruit collapse by day 30. In contrast, coated samples better preserved their morphology, with sericin-containing films (SerAlg1 and SerAlg2) showing less surface deterioration than alginate alone (SerAlg0). The incorporation of RC extract further contributed to maintaining fruit integrity, particularly in formulations with higher sericin content. Under refrigerated storage (4 °C, Fig. 9B), all fruits exhibited improved visual appearance compared to those storage at R.T. Coated blueberries showed delayed shriveling and smoother surfaces after 30 days, with SerAlg2 and SerAlgRC2 maintaining the most preserved morphology. These observations are consistent with the WVTR results (Table 1, Fig. 6), which demonstrated that increasing sericin content reduced the water vapor permeability of the films. Lower WVTR limits transpiration and promotes moisture retention within the fruit, thereby reducing dehydration and surface wrinkling.

After harvest, fruits lose weight during storage due to transpiration and respiration. Water loss leads to weight reduction, external changes, and surface shrinkage, ultimately shortening shelf life. To evaluate the effectiveness of the coatings in preserving blueberry quality, Figs. 10 and 11 show the time-dependent weight loss of blueberries (expressed as a fraction of their original weight) stored at R.T. and under refrigeration (4 °C), respectively. Uncoated control samples are included for

comparison. At R.T. (Fig. 10A), after 5 days, blueberries coated with sericin-based films without RC extract retained less than 80% of their original weight, whereas those coated with RC extract retained slightly more (Fig. 10B). Among the formulations, SerAlg2 and SerAlgRC2 maintained the highest fraction of their original weight throughout the storage period, with values of  $34.60 \pm 2.00\%$  and  $28.60 \pm 2.76\%$ , respectively, after 30 days. Under refrigeration (4 °C) (Fig. 11), all blueberries, both with and without RC extract, retained a higher fraction of their original weight compared with R.T. storage (Fig. 10). After 30 days, SerAlg2 and SerAlgRC2 retained  $74.99 \pm 7.20\%$  and  $66.27 \pm 2.62\%$  of their original weight, respectively. The results showed that blueberries coated with sericin containing RC extract exhibited higher weight loss than those coated with sericin alone at both temperatures. This behavior is likely due to the higher swelling ratio of the RC-containing coating, which increases water uptake and permeability, thereby reducing its effectiveness as a barrier to water loss.~

### 3.10. Smart packaging

Photographs of sericin-alginate films containing RC extract in buffer solutions of varying pH are shown in Fig. 12. All films exhibited visible color changes due to the presence of anthocyanins, shifting from purple (pH = 2) to blue (pH = 7), green (pH = 10), and yellow (pH = 12). Notably, films incorporating sericin (SerAlgRC1 and SerAlgRC2) displayed more intense coloration compared with the base formulation (SerAlgRC0). This observation is consistent with recent studies reporting that proteins can protect and stabilize anthocyanins (Y. Yang et al., 2025).

Although the films clearly responded to pH changes in buffer solutions, no significant color changes were observed in blueberries coated with RC extract after 30 days of storage. This may be due to the limited release of volatile compounds capable of inducing significant pH changes during blueberry storage. As a future perspective, the intelligent packaging system could be tested with meat or fish products, which are known to release ammonia (NH<sub>3</sub>) and biogenic amines during spoilage (Jamróz et al., 2019). These volatile compounds are more likely to cause detectable pH change, potentially triggering a visible response in the anthocyanin-based indicator.

## 4. Conclusions

Smart edible films were successfully developed by incorporating sericin and RC extract into an alginate matrix. RC extract significantly altered film color, with total color differences ( $\Delta E^*$ ) up to 33.98, while sericin modulated lightness and opacity. Structural analyses showed that sericin and RC phenolics increased film thickness and density, enhancing intermolecular interactions. Mechanical properties depended on composition: moderate sericin improved TS and YM, whereas higher sericin increased stiffness and reduced extensibility, while RC extract generally enhanced flexibility. Water vapor transmission decreased with

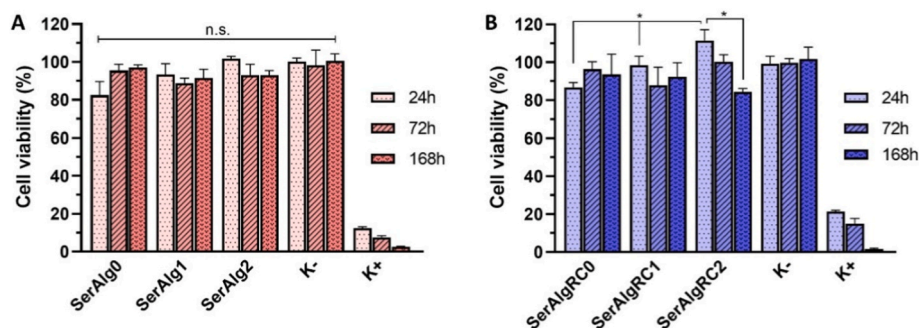


Fig. 8. Characterization of the cytotoxic profile of the sericin-alginate films without (A) and with RC extract (B), n = 3. Data are presented as mean  $\pm$  standard deviation, n.s.-not statistically significant, and \* $p < 0.05$ .

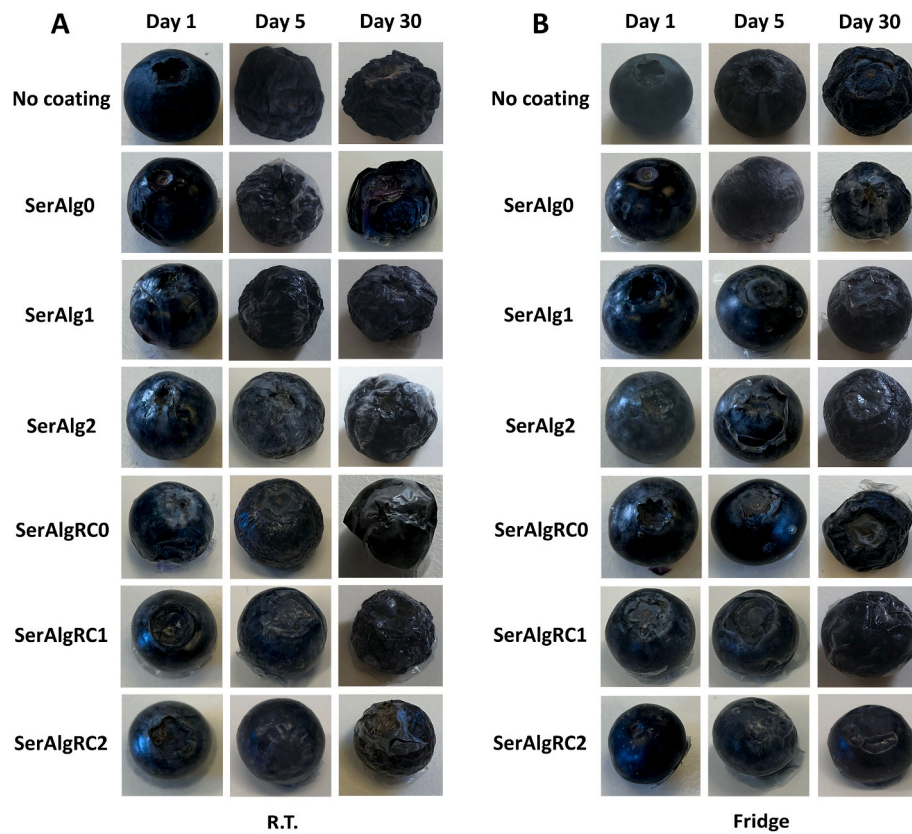


Fig. 9. Photographs of blueberries ripening without and with edible coating during 30 days of storage at room temperature (R.T.) (A) and under refrigeration (4 °C) (B).

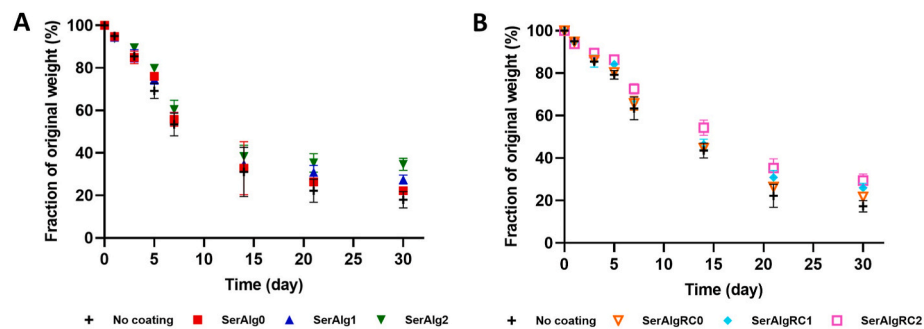


Fig. 10. Weight loss of blueberries stored for 30 days at room temperature. Blueberries were stored with no coating) or after coating with sericin-based film without (A) and with RC extract (B).

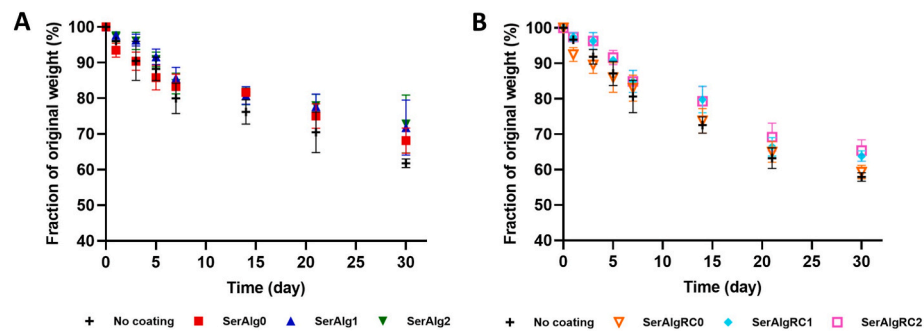


Fig. 11. Weight loss of blueberries stored for 30 days in the refrigerator (4 °C). Blueberries were stored uncoated or coated with sericin-based films without (A) or with RC extract (B).

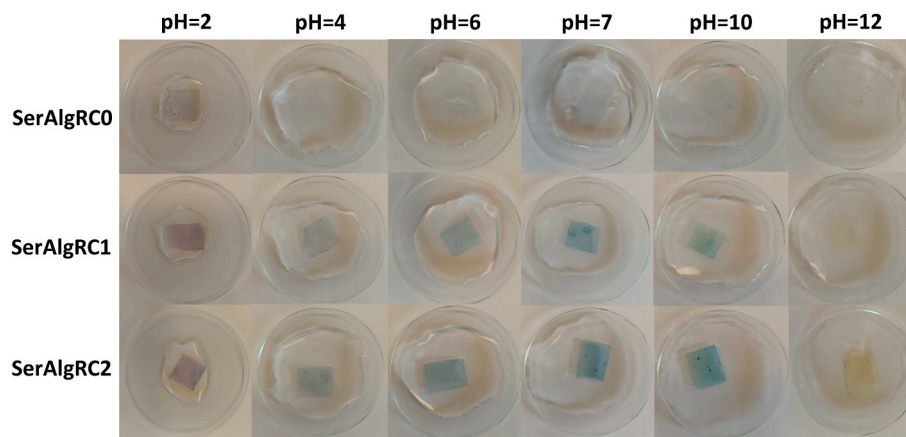


Fig. 12. Color change of sericin–alginate films containing RC extract after immersion in solutions of different pH values.

higher sericin and RC content, and swelling capacity increased, reflecting enhanced hydrophilicity. Coatings effectively reduced blueberry dehydration and preserved fruit morphology during storage, although no visible pH-responsive color changes occurred on the fruit, likely due to the minimal release of volatile compounds capable of altering pH. Cytotoxicity assays confirmed the films' safety. By valorising sericin, this approach aligns with circular economy principles and offers a sustainable alternative to conventional packaging. Future studies should apply these films/coatings in foods where pH variations are more pronounced to fully exploit their smart functionality.

#### CRedit authorship contribution statement

**Daniela Pinheiro:** Writing – review & editing, Writing – original draft, Visualization, Validation, Supervision, Methodology, Investigation, Formal analysis, Data curation, Conceptualization. **Ana Rita Ferraz:** Writing – original draft, Visualization, Validation, Supervision, Methodology, Investigation, Formal analysis, Data curation. **Sofia Esteves:** Methodology, Investigation, Data curation. **Ofélia Anjos:** Writing – review & editing, Validation, Formal analysis. **Maximiano P. Ribeiro:** Writing – review & editing, Visualization, Validation, Supervision, Project administration, Funding acquisition, Conceptualization.

#### Declaration of competing interest

The authors declare that they have no known competing financial interests or personal relationships that could have appeared to influence the work reported in this paper.

#### Acknowledgments

The authors acknowledge the Portuguese Foundation for Science and Technology (FCT) for financial support to the Research Centre for Natural Resources, Environment and Society - CERNAS (UID/00681/2025, <https://doi.org/10.54499/UID/00681/2025>), and Biotechnology Research, Innovation and Design for Health Products - BRIDGES (UID/PRR/06407/2025 and UID/06407/2025, <https://doi.org/10.54499/UID/06407/2025>). This work was carried out within the scope of the project “WASTESILK - Silk Sericin as an Industrial Wastewater with Valuable Biomedical Potential” (PTDC/BTA-BTA/0696/2020), funded by national funds through FCT. D. Pinheiro also acknowledges WASTESILK for the research contract (CO.IPG.2023.1373).

#### Appendix A. Supplementary data

Supplementary data to this article can be found online at <https://doi.org/10.1016/j.fbio.2026.108488>.

#### Data availability

Data will be made available on request.

#### References

- Aad, R., Dragojlov, I., & Vesentini, S. (2024). Sericin protein: Structure, properties, and applications. *Journal of Functional Biomaterials*, 15(11), 322. <https://doi.org/10.3390/jfb15110322>
- Abedi-Firoozjah, R., Yousefi, S., Heydari, M., Seyedfatehi, F., Jafarzadeh, S., Mohammadi, R., ... Garavand, F. (2022). Application of red cabbage anthocyanins as pH-Sensitive pigments in smart food packaging and sensors. *Polymers*, 14(8), 1629. <https://doi.org/10.3390/polym14081629>
- Al-Harrasi, A., Bhtaia, S., Al-Azri, M. S., Makeen, H. A., Albratty, M., Alhazmi, H. A., ... Behl, T. (2022). Development and characterization of chitosan and porphyrin based composite edible films containing ginger essential oil. *Polymers*, 14(9), 1782. <https://doi.org/10.3390/polym14091782>
- Alves Lopes, I., Coelho Paixão, L., Souza da Silva, L. J., Almeida Rocha, A., Barros Filho, A. K. D., & Amorim Santana, A. (2020). Elaboration and characterization of biopolymer films with alginate and babassu coconut mesocarp. *Carbohydrate Polymers*, 234, Article 115747. <https://doi.org/10.1016/j.carbpol.2019.115747>
- Apiwattanasiri, P., Charoen, R., Rittisak, S., Phattayakorn, K., Jantrasee, S., & Savedboworn, W. (2022). Co-encapsulation efficiency of silk sericin-alginate-prebiotics and the effectiveness of silk sericin coating layer on the survival of probiotic *Lactobacillus casei*. *Food Bioscience*, 46, Article 101576. <https://doi.org/10.1016/j.fbio.2022.101576>
- Aramwit, P., Damrongsakkul, S., Kanokpanont, S., & Srichana, T. (2010). Properties and antityrosinase activity of sericin from various extraction methods. *Biotechnology and Applied Biochemistry*, 55(2), 91–98. <https://doi.org/10.1042/BA20090186>
- Arango, M. C., Montoya, Y., Peresin, M. S., Bustamante, J., & Álvarez-López, C. (2021). Silk sericin as a biomaterial for tissue engineering: A review. *ISBPPB*, 70(16), 1115–1129. <https://doi.org/10.1080/00914037.2020.1785454>
- Arshad, M. T., Hassan, S., Shehzadi, R., Sani, M. A., Ikram, A., Maqsood, S., ... Gnedeka, K. T. (2025). Emerging trends in sustainable packaging of food products: An updated review. *Journal of Natural Fibers*, 22(1), Article 2505608. <https://doi.org/10.1080/15440478.2025.2505608>
- Atta, O. M., Manan, S., Shahzad, A., Ul-Islam, M., Ullah, M. W., & Yang, G. (2022). Biobased materials for active food packaging: A review. *Food Hydrocolloids*, 125, Article 107419. <https://doi.org/10.1016/j.foodhyd.2021.107419>
- Bascou, R., Hardouin, J., Ben Mlouka, M. A., Guénin, E., & Nesterenko, A. (2022). Detailed investigation on new chemical-free methods for silk sericin extraction. *Materials Today Communications*, 33, Article 104491. <https://doi.org/10.1016/j.mtcomm.2022.104491>
- Bayram, B., Ozkan, G., Kostka, T., Capanoglu, E., & Esatbeyoglu, T. (2021). Valorization and application of fruit and vegetable wastes and By-Products for food packaging materials. *Molecules*, 26(13), 4031. <https://doi.org/10.3390/molecules26134031>
- Behrooznia, Z., & Nourmohammadi, J. (2024). Polysaccharide-based materials as an eco-friendly alternative in biomedical, environmental, and food packaging. *Giant*, 19, Article 100301. <https://doi.org/10.1016/j.giant.2024.100301>
- Bishnoi, S., Trifol, J., Moriana, R., & Mendes, A. C. (2022). Adjustable polysaccharides-proteins films made of aqueous wheat proteins and alginate solutions. *Food Chemistry*, 391, Article 133196. <https://doi.org/10.1016/j.foodchem.2022.133196>
- Bof, M. J., Laurent, F. E., Massolo, F., Locaso, D. E., Versino, F., & García, M. A. (2021). Bio-packaging material impact on blueberries quality attributes under transport and marketing conditions. *Polymers*, 13(4), 481. <https://doi.org/10.3390/polym13040481>
- Chentir, I., Aribi, C., Tarchoun, A. F., Kchaou, H., Lamri, M., Nasri, M., & Trache, D. (2024). Development of functional active films from blend of gelatin with crude Orange juice pomace pectin: Test for packaging of virgin olive oil. *Packaging Technology and Science*, 37(1), 17–37. <https://doi.org/10.1002/pts.2776>

- Chimvaree, C., Wongs-Aree, C., Supapvanich, S., Charoenrat, T., Tepsorn, R., & Boonyarittongchai, P. (2019). Effect of sericin coating on reducing browning of fresh-cut mango cv. 'Nam Dok Mai No. 4'. *Agr. Nat. Resour.*, (53), 521–526. <https://doi.org/10.34044/jv.anres.2019.53.5.11>
- Dou, L., Li, B., Zhang, K., Chu, X., & Hou, H. (2018). Physical properties and antioxidant activity of gelatin-sodium alginate edible films with tea polyphenols. *International Journal of Biological Macromolecules*, 118, 1377–1383. <https://doi.org/10.1016/j.ijbiomac.2018.06.121>
- Ghareaghajlou, N., Hallaj-Nezhadi, S., & Ghasempour, Z. (2021). Red cabbage anthocyanins: Stability, extraction, biological activities and applications in food systems. *Food Chemistry*, 365, Article 130482. <https://doi.org/10.1016/j.foodchem.2021.130482>
- Gupta, D., Agrawal, A., & Rangi, A. (2014). Extraction and characterization of silk sericin. *Indian J Fibre Text Res*, 39, 364–372.
- Hailu, G. T., Alemea, M. T., & Lemessa, F. (2025). Development of silk sericin-based polysaccharide-protein hybrid biofilms: Mechanical, thermal, and antibacterial properties. *Research: Ideas for Today's Investors*, 2(2), Article 100097. <https://doi.org/10.1016/j.nexres.2024.100097>, 1.
- Hossain, S., Ali, R., & Hasan, T. (2023). Extraction and characterization of sericin from cocoon of four different silkworm races *Bombyx mori* L. *European J. Adv. Chem. Res*, 4(3), 45–52. <https://doi.org/10.24018/ejchem.2023.4.3.134>
- Huang, X., Nakagawa, S., Houjou, H., & Yoshie, N. (2021). Insights into the role of hydrogen bonds on the mechanical properties of polymer networks. *Macromolecules*, 54(9), 4070–4080. <https://doi.org/10.1021/acs.macromol.1c00120>
- Hussain, S., Akhter, R., & Maktedar, S. S. (2024). Advancements in sustainable food packaging: From eco-friendly materials to innovative technologies. *Sustain. Food Technol*, 2(5), 1297–1364. <https://doi.org/10.1039/d4fb00084f>
- Iqbal, S., Ayyub, A., Bhutto, R. A., & Rehman, W. (2025). Designing smart and sustainable edible packaging materials from biopolymers, proteins, and polysaccharides. In S.u. Islam, & M. Shahid (Eds.), *Green materials for active food packaging* (pp. 131–196). Singapore: Springer Nature Singapore.
- Jamroz, E., Kulawik, P., Guzik, P., & Duda, I. (2019). The verification of intelligent properties of furcellaran films with plant extracts on the stored fresh Atlantic mackerel during storage at 2 °C. *Food Hydrocolloids*, 97, Article 105211. <https://doi.org/10.1016/j.foodhyd.2019.105211>
- Jaya Prakash, N., Shanmugarajan, D., Wang, X., & Kandasubramanian, B. (2022). Enhancement of mechano-structural characteristics of silk fibroin using microwave assisted degumming. *Sustainable Chemistry and Pharmacy*, 30, Article 100902. <https://doi.org/10.1016/j.scp.2022.100902>
- Kavi, P., Tarangini, K., Kumaravel, V., Rao, K. J., Waclawek, S., Cheong, J. Y., & Padil, V. V. T. (2024). Multifunctional sericin-chitosan-aloe vera composite film for food packaging. *Ecol Chem Eng S*, 31(3), 297–314. <https://doi.org/10.2478/eces-2024-0020>
- Khan, A., Riahi, Z., Tae Kim, J., & Rhim, J.-W. (2024). Carrageenan-based multifunctional packaging films containing Zn-carbon dots/anthocyanin derived from kohlrabi peel for monitoring quality and extending the shelf life of shrimps. *Food Chemistry*, 432, Article 137215. <https://doi.org/10.1016/j.foodchem.2023.137215>
- Kossvyaki, D., Contardi, M., Athanassiou, A., & Fragouli, D. (2022). Colorimetric indicators based on anthocyanin/polymer composites: A review. *Polymers*, 14(19), 4129. <https://doi.org/10.3390/polym14194129>
- Kumar, R., Lalnundiki, V., Shelare, S. D., Abhishek, G. J., Sharma, S., Sharma, D., ... Abbas, M. (2024). An investigation of the environmental implications of bioplastics: Recent advancements on the development of environmentally friendly bioplastics solutions. *Environmental Research*, 244, Article 117707. <https://doi.org/10.1016/j.envres.2023.117707>
- Kuswandi, B., Asih, N. P. N., Pratoko, D. K., Kristiningrum, N., & Moradi, M. (2020). Edible pH sensor based on immobilized red cabbage anthocyanins into bacterial cellulose membrane for intelligent food packaging. *Packaging Technology and Science*, 33(8), 321–332. <https://doi.org/10.1002/pts.2507>
- Li, H., Liu, C., Sun, J., & Lv, S. (2022). Bioactive edible sodium alginate films incorporated with tannic acid as antimicrobial and antioxidant food packaging. *Food*, 11(19), 3044. <https://doi.org/10.3390/foods11193044>
- Maftoonazad, N., & Ramaswamy, H. (2019). Design and testing of an electrospun nanofiber mat as a pH biosensor and monitor the pH associated quality in fresh date fruit (rutab). *Polym. Testing*, 75, 76–84. <https://doi.org/10.1016/j.polymertesting.2019.01.011>
- Meerasri, J., Sukatta, U., Rugthaworn, P., Klinsukhon, K., Khacharat, L., Sakayaroj, S., ... Sothernvit, R. (2024). Synergistic effects of thyme and oregano essential oil combinations for enhanced functional properties of sericin/pectin film. *International Journal of Biological Macromolecules*, 263, Article 130288. <https://doi.org/10.1016/j.ijbiomac.2024.130288>
- Metha, C., Pawar, S., & Suvarna, V. (2024). Recent advancements in alginate-based films for active food packaging applications. *Sustain. Food Technol*, 2(5), 1246–1265. <https://doi.org/10.1039/D3FB00216K>
- Miguel, S. P., D'Angelo, C., Ribeiro, M. P., Ferreira, S., & Coutinho, P. (2023). An antibacterial and bioactive sponge incorporating codium sp.-mediated biosynthesized silver nanoparticles for the management of high exudate wounds. *Algal Research*, 72, Article 103129. <https://doi.org/10.1016/j.algal.2023.103129>
- Miguel, S. P., Ribeiro, M. P., Coutinho, P., & Correia, I. J. (2017). Electrospun polycaprolactone/aloe vera Chitosan nanofibrous asymmetric membranes aimed for wound healing applications. *Polymers*, 9(5), 183. <https://doi.org/10.3390/polym9050183>
- Nechita, P., & Roman, M. (2020). Review on polysaccharides used in coatings for food packaging papers. *Coatings*, 10(6), 566. <https://doi.org/10.3390/coatings10060566>
- Oh, S., Park, J., Nam, J., Hyun, Y., Jin, H.-J., & Kwak, H. W. (2021). Antioxidant and UV-blocking glucose-crosslinked sericin films with enhanced structural integrity. *React Funct Polym*, 165, Article 104942. <https://doi.org/10.1016/j.reactfunctpolym.2021.104942>
- Oladzadabbasabadi, N., Mohammadi Nafchi, A., Ghasemlou, M., Ariffin, F., Singh, Z., & Al-Hassan, A. A. (2022). Natural anthocyanins: Sources, extraction, characterization, and suitability for smart packaging. *Food Packaging and Shelf Life*, 33, Article 100872. <https://doi.org/10.1016/j.foodpsl.2022.100872>
- Otoni, C. G., Avena-Bustillos, R. J., Azeredo, H. M. C., Lorevice, M. V., Moura, M. R., Mattoso, L. H. C., & McHugh, T. H. (2017). Recent advances on edible films based on fruits and vegetables—A review. *Comprehensive Reviews in Food Science and Food Safety*, 16(5), 1151–1169. <https://doi.org/10.1111/1541-4337.12281>
- Pan, M., Jin, Y., Ye, Y., Jiang, W., Zhu, L., & Lu, W. (2024). An efficient and eco-friendly method for removing sericin using microwave-assisted steam degumming. *Environmental Technology & Innovation*, 35, Article 103674. <https://doi.org/10.1016/j.eti.2024.103674>
- Pan, J., Li, C., Liu, J., Jiao, Z., Zhang, Q., Lv, Z., ... Liu, H. (2024). Polysaccharide-Based packaging coatings and films with phenolic compounds in preservation of fruits and Vegetables-A review. *Foods*, 13(23). <https://doi.org/10.3390/foods13233896>
- Pandey, V., Sharma, A., Sharma, A., & Kumari, V. (2024). The role of silk as natural biomaterial in food safety. *Food Bioscience*, 60, Article 104538. <https://doi.org/10.1016/j.fbio.2024.104538>
- Pourjavaher, S., Almasi, H., Meshkini, S., Pirsas, S., & Parandi, E. (2017). Development of a colorimetric pH indicator based on bacterial cellulose nanofibers and red cabbage (*Brassica oleracea*) extract. *Carbohydrate Polymers*, 156, 193–201. <https://doi.org/10.1016/j.carbpol.2016.09.027>
- Qin, Y., Liu, Y., Yong, H., Liu, J., Zhang, X., & Liu, J. (2019). Preparation and characterization of active and intelligent packaging films based on cassava starch and anthocyanins from *Lycium ruthenicum murr.* *International Journal of Biological Macromolecules*, 134, 80–90. <https://doi.org/10.1016/j.ijbiomac.2019.05.029>
- Riaz, A., Lei, S., Akhtar, H. M. S., Wan, P., Chen, D., Jabbar, S., ... Zeng, X. (2018). Preparation and characterization of chitosan-based antimicrobial active food packaging film incorporated with apple peel polyphenols. *International Journal of Biological Macromolecules*, 114, 547–555. <https://doi.org/10.1016/j.ijbiomac.2018.03.126>
- Rodrigues, D. A., Miguel, S. P., Loureiro, J., Ribeiro, M., Roque, F., & Coutinho, P. (2021). Oromucosal alginate films with zein nanoparticles as a novel delivery system for digoxin. *Pharmaceutics*, 13(12), 2030. <https://doi.org/10.3390/pharmaceutics13122030>
- Roy, S., & Rhim, J.-W. (2021). Anthocyanin food colorant and its application in pH-responsive color change indicator films. *Critical Reviews in Food Science and Nutrition*, 61(14), 2297–2325. <https://doi.org/10.1080/10408398.2020.1776211>
- Saad, M., El-Samad, L. M., Gomaa, R. A., Augustyniak, M., & Hassan, M. A. (2023). A comprehensive review of recent advances in silk sericin: Extraction approaches, structure, biochemical characterization, and biomedical applications. *International Journal of Biological Macromolecules*, 250, Article 126067. <https://doi.org/10.1016/j.ijbiomac.2023.126067>
- Saha, J., Mondal, M. I. H., Sheikh, M. R. K., & Karim, M. R. (2019). Extraction, structural and functional properties of silk sericin biopolymer from *Bombyx mori* silk cocoon waste. *J Textile Sci Eng*, 9(1), 2165–8064. <https://doi.org/10.4172/2165-8064.1000390>
- Seo, S.-J., Das, G., Shin, H.-S., & Patra, J. K. (2023). Silk sericin protein materials: Characteristics and applications in food-sector industries. *International Journal of Molecular Sciences*, 24(5), 4951. <https://doi.org/10.3390/ijms24054951>
- Shi, D., Zhao, B., Zhang, P., Li, P., Wei, X., & Song, K. (2024). Edible composite films: Enhancing the postharvest preservation of blueberry. *Hortic Environ Biotechnol*, 65(3), 355–373. <https://doi.org/10.1007/s13580-023-00581-4>
- Silva, V. R., Ribani, M., Gimenes, M. L., & Scheer, A. P. (2012). High molecular weight sericin obtained by high temperature and ultrafiltration process. *Procedia Engineering*, 42, 833–841. <https://doi.org/10.1016/j.proeng.2012.07.476>
- Sothernvit, R., & Chollakup, R. (2009). Properties of sericin-glucomannan composite films. *International Journal of Food Science and Technology*, 44(7), 1395–1400. <https://doi.org/10.1111/j.1365-2621.2009.01969.x>
- Suresh, S. N., Puspharaj, C., Natarajan, A., & Subramani, R. (2022). Gum acacia/pectin/pullulan-based edible film for food packaging application to improve the shelf-life of ivy gourd. *International Journal of Food Science and Technology*, 57(9), 5878–5886. <https://doi.org/10.1111/ijfs.15909>
- Tarangini, K., Kavi, P., & Jagajjanani Rao, K. (2022). Application of sericin-based edible coating material for postharvest shelf-life extension and preservation of tomatoes. *eFood*, 3(5), e36. <https://doi.org/10.1002/efd2.36>
- Wang, J., Shang, J., Ren, F., & Leng, X. (2010). Study of the physical properties of whey protein: Sericin protein-blended edible films. *European Food Research and Technology*, 231(1), 109–116. <https://doi.org/10.1007/s00217-010-1259-x>
- Yang, Y., Chen, L., Chen, M., Liu, F., & Zhong, F. (2025). Interactions between rice protein and anthocyanin with different pH-cycle: Structural characterization, binding mechanism and stability. *Food Hydrocolloids*, 165, Article 111230. <https://doi.org/10.1016/j.foodhyd.2025.111230>
- Yang, C., Yao, L., & Zhang, L. (2023). Silk sericin-based biomaterials shine in food and pharmaceutical industries. *SMART*, 4, 447–459. <https://doi.org/10.1016/j.smaim.2023.01.003>
- Yong, H., & Liu, J. (2020). Recent advances in the preparation, physical and functional properties, and applications of anthocyanins-based active and intelligent packaging films. *Food Packaging and Shelf Life*, 26, Article 100550. <https://doi.org/10.1016/j.foodpsl.2020.100550>
- Zhai, X., Shi, J., Zou, X., Wang, S., Jiang, C., Zhang, J., ... Holmes, M. (2017). Novel colorimetric films based on starch/polyvinyl alcohol incorporated with roselle

- anthocyanins for fish freshness monitoring. *Food Hydrocolloids*, 69, 308–317. <https://doi.org/10.1016/j.foodhyd.2017.02.014>
- Zhang, Z., Wang, Y., Fang, X., Chen, X., Yin, Z., & Zhang, C. (2024). Preparation of edible film from sweet potato peel polyphenols: Application in fresh fruit preservation. *Frontiers in Sustainable Food Systems*, 8–2024. <https://doi.org/10.3389/fsufs.2024.1470732>
- Zhou, W., Duan, Z., Zhao, J., Fu, R., Zhu, C., & Fan, D. (2022). Glucose and MMP-9 dual-responsive hydrogel with temperature sensitive self-adaptive shape and controlled drug release accelerates diabetic wound healing. *Bioactive Materials*, 17, 1–17. <https://doi.org/10.1016/j.bioactmat.2022.01.004>